Rejuvenation and memory effects in active glasses induced by thermal and active cycling

Giulia Janzen and Liesbeth M. C. Janssen*

Department of Applied Physics, Eindhoven University of Technology, P.O. Box 513, 5600 MB Eindhoven, The Netherlands

(Received 9 August 2023; accepted 26 April 2024; published 7 June 2024)

It has recently been shown that thermal active glasses can display physical aging behavior comparable to that of passive glasses, although there are some notable distinctions due to the intrinsic nonequilibrium nature of active matter. The question whether active disordered materials can also exhibit rejuvenation and memory effects, akin to the phenomenology of, e.g., spin glasses, has thus far remained unexplored. Here we address this question by numerical simulations of active glasses composed of active Brownian particles that are subjected to a thermal or active cycling protocol. We find that an active system undergoing thermal cycling indeed shows rejuvenation and memory effects, with the strength of rejuvenation depending on the persistence time. In contrast, however, a passive Brownian system subjected to the same thermal cycle lacks the rejuvenation effect. We attribute this to the enhanced motility of active particles, which enables them to escape from their cages and restart aging at the new temperature, thus rejuvenating the material. Finally, we also demonstrate that both rejuvenation and memory effects can be induced by an activity cycle which quenches the material from an active to passive glass and back, providing a unique means to rejuvenate active matter.

DOI: 10.1103/PhysRevResearch.6.023257

I. INTRODUCTION

The dynamics of many densely disordered systems, i.e., glassy materials, is characterized by an extremely slow structural relaxation that is often explicitly dependent on the age of the material. This age (or waiting time) dependence is called physical aging and is particularly well studied for glasses following a sudden quench toward a lower temperature [1–4]. After such a temperature quench, the structural relaxation time tends to increase with the age of the material, typically as a power law [5–15]. Theoretically, this aging behavior can be understood as a gradual approach of the material toward lower-energy equilibrium states [3,7,16]. While a single thermal quench is one of the most popular protocols to study the aging behavior of glassy systems, other protocols, such as thermal cycling involving repeated temperature changes, may lead to even richer dynamical behaviors and offer more versatility to characterize a material's out-of-equilibrium dynamics.

For spin glasses, the effect of thermal cycling has been studied theoretically, experimentally, and in numerical simulations, disclosing new insights into their dynamical behavior [17–34]. As shown in Fig. 1, the protocol consists of three steps: firstly, a high-temperature liquid is cooled to $T_{q_1} < T_g$ (where T_g is the glass transition temperature); after a certain interval, the temperature is quenched once more to a lower temperature $T_{q_2} < T_{q_1}$; and finally, the temperature is reheated to T_{q_1} [27,35,36]. During the first step, the system undergoes aging. In the subsequent step, instead of the relaxation process slowing down further, the aging process restarts at the new temperature T_{q_2}. This phenomenon is referred to as "rejuvenation" [27,35]. More explicitly, the relaxation at T_{q_2} will be identical to that obtained from a direct quench at this temperature if the temperature jump $\Delta T = |T_{q_1} - T_{q_2}|$ is sufficiently large [22,25,30,33,37], thus implying that an old glass behaves dynamically as a young glass at a lower temperature. Hence, in this case the old glass has been "rejuvenated" [27,34–36]. We note that rejuvenation can be also studied using positive temperature shifts involving a heating of the system to temperatures higher than T_{q_1} [38], but here we follow the definition of Refs. [34–36]. In the third step of the thermal cycling protocol, when the temperature is brought back to T_{q_1}, the system exhibits *full memory* if the relaxation restarts exactly from the point reached before the second step (i.e., such that the time-dependent relaxation dynamics effectively picks up from where it ended after the first step). However, achieving full memory requires a sufficiently large temperature difference, denoted as ΔT. If ΔT is not large enough, the behavior observed in the third step will be influenced by the aging that occurred at T_{q_2} [35,39].

Several studies have explored whether rejuvenation and memory, as observed in spin glasses, can also occur in structural glasses. Recent computer simulations of a continuously polydisperse model glass former have shown that temperature cycling indeed leads to rejuvenation and memory effects, provided that both the duration of each step in the cycle and the temperature jumps between the steps are sufficiently large [36]. Similarly, in numerical simulations of binary Lennard-Jones mixtures, it was found that oscillatory temperature variations may induce rejuvenation, depending on the cooling rate and cycling amplitude [40,41]. Numerous studies have also explored emergent nonequilibrium phenomena in metallic glasses exposed to oscillatory temperature variations [42–44]. Most notably, subjecting metallic glasses to

*l.m.c.janssen@tue.nl

Published by the American Physical Society under the terms of the Creative Commons Attribution 4.0 International license. Further distribution of this work must maintain attribution to the author(s) and the published article's title, journal citation, and DOI.

cryogenic thermal cycling can induce rejuvenation and improve the plasticity of the material [45–47].

The study of glassy phenomena has recently seen a renewed surge of interest through the advent of active matter, i.e., nonequilibrium systems composed of self-propelling particles. Both theory and simulations [48–60], as well as experiments [61–71], have shown that dense active matter shares many similarities with conventional glassy systems, including anomalously slow dynamics and aging. It is important to note, however, that the conventional understanding of physical aging in passive glasses, where the material tends to reach equilibrium through energy minimization, does not hold for active glasses. This is because active systems are non-Hamiltonian systems, inherently far from equilibrium, making it unclear *a priori* how these systems will undergo aging. Thus far the physical aging behavior of active systems has been explored in a small number of simulation studies for thermal [72] and athermal active glasses [73,74] using a single temperature quench, a change in density, or a single activity quench, respectively. Notably, for active thermal glasses, the aging relaxation dynamics was found to be governed by a time-dependent competition between thermal and active effects, with the active particles' persistence time controlling both the timescale and magnitude of the activity-enhanced speedup in dynamics [72]. However, it remains unclear how a protocol such as a thermal cycle would impact the dynamics of an active glass and whether activity itself could be used to design a new nonequilibrium protocol, such as an activity cycle.

Here we investigate how cyclic protocols affect the dynamics of structural active glasses. We find that, in contrast to our passive reference sample, active glasses do exhibit rejuvenation under a simple temperature cycle. Importantly, the strength of this thermally induced rejuvenation effect depends on the active particles' persistence time. We also observe a clear memory effect that, unlike rejuvenation, is more easily observed and independent of the persistence time. Moreover, we introduce a cyclic protocol unique to active matter in which an active sample is made passive and then active again. By applying this protocol, we find that the rich out-of-equilibrium dynamics observed in the temperature cycle protocol becomes even more pronounced in the activity cycle.

II. METHODS

A. Simulation model

We study a two-dimensional (2D) binary mixture of thermal active Brownian particles (ABPs). The overdamped equations of motion for each particle i are given by

$$\gamma \dot{\boldsymbol{r}}_i = \sum_{i\neq j=1}^{N} \boldsymbol{f}_{ij} + f\,\boldsymbol{n}_i + \sqrt{2D_T}\,\boldsymbol{\eta}, \tag{1}$$

$$\dot{\theta}_i = \sqrt{2D_r}\,\eta_\theta, \tag{2}$$

where $\boldsymbol{r}_i = (x_i, y_i)$, and θ_i represent the particle's spatial and rotational coordinates, respectively. The dots denote a time derivative. Thermal noise is modeled as an independent Gaussian stochastic process, $\boldsymbol{\eta} = (\eta_x, \eta_y)$, with zero mean and variance $2D_T\delta(t-t')$, where $D_T = k_BT/\gamma$ with k_B being the Boltzmann constant, T the temperature, and γ the friction coefficient. The rotational noise η_θ is a Gaussian stochastic process with zero mean and variance $2D_r\delta(t-t')$. The factors D_T and D_r represent the translational and rotational diffusion constants, respectively, and the ABP persistence time is defined as $\tau_r = D_r^{-1}$. The constant self-propulsion speed f/γ is applied to each ABP along a direction $\boldsymbol{n}_i = (\cos\theta_i, \sin\theta_i)$. Note that when the active force f is equal to zero, Eq. (1) reduces to the equation of motion for a passive Brownian particle. Finally, $\boldsymbol{f}_{ij} = -\nabla_i V(r_{ij})$ is the interaction force between particles i and j, where $r_{ij} = |\mathbf{r}_i - \mathbf{r}_j|$ and V is the Lennard-Jones potential with a cutoff distance $r_{ij} = 2.5\sigma_{ij}$ and zero otherwise. In order to prevent crystallization, we use the parameters of the 2D binary Kob-Andersen mixture [75]: $A = 65\%$, $B = 35\%$, $\epsilon_{AA} = 1$, $\epsilon_{BB} = 0.5\epsilon_{AA}$, $\epsilon_{AB} = 1.5\epsilon_{AA}$, $\sigma_{AA} = 1$, $\sigma_{BB} = 0.88\sigma_{AA}$, and $\sigma_{AB} = 0.8\sigma_{AA}$. We set the density to $\rho = 1.2$, the number of particles to $N = 10\,000$, and $D_T = \gamma = 1$. Results are in reduced units, where σ_{AA}, ϵ_{AA}, $\frac{\sigma_{AA}^2\gamma}{\epsilon_{AA}}$, and $\frac{\epsilon_{AA}}{k_B}$ are the units of length, energy, time, and temperature, respectively. Simulations were performed using LAMMPS [76] by solving Eqs. (1) and (2) via the Euler-Maruyama method with a step size $\delta t = 10^{-4}$.

B. Protocols

To induce possible rejuvenation and memory effects, we expose our system to two different protocols: thermal and active cycling. The thermal cycling protocol is applied to both an active system ($f = 0.5$ and $\tau_r = 1, 10$) and a passive system ($f = 0$) for comparison. In both cases we prepare 1000 independent configurations, which we first allow to equilibrate at a high temperature $T_i = 1$. We note that this relatively large number of independent trajectories is needed to ensure sufficient statistical quality of the results. Once the equilibration process is completed, we quench the temperature below the glass transition temperature to $T_{q_1} = 0.25 < T_g$, where T_g is approximately 0.4 or 0.3 for a passive and active system, respectively [72,77,78]. The system is then allowed to evolve at T_{q_1} for a duration of t_1. This initial aging step is followed by another quench to $T_{q_2} = 0.1 < T_{q_2}$, after which the system is allowed to evolve for a time t_2. Finally, we increase the temperature back to T_{q_1} and allow the system to evolve for a duration of t_3. After some testing, we have found that $t_1 = t_2 = t_3 = 500$ or 1000 provides a reasonable time frame to probe possible rejuvenation and memory effects. The left axis of Fig. 1 illustrates the temperature cycle protocol used in our simulations.

For the activity cycling protocol, we control the active system's behavior by quenching the persistence time τ_r. To achieve this, we prepare 1000 independent configurations at a temperature of $T = 0.1$ or 0.25 and an active force of $f = 0.5$. We then equilibrate the system at a high persistence time of $\tau_{r_i} = 100$ before quenching the persistence time to $\tau_{r_1} = 10$. We subsequently allow the system to evolve for a time interval t_1. After this initial aging step, we quench the persistence time once again to $\tau_{r_2} = 0$ to obtain a passive system. The system then evolves for a time t_2. Finally, we change the persistence time back to $\tau_{r_1} = 10$, and we let the system evolve for a time interval of t_3 (right axis of Fig. 1). In all cases we

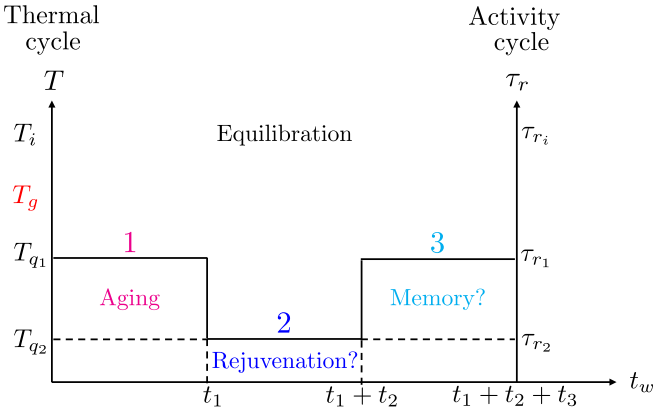


FIG. 1. Cyclic protocols used in this work to induce aging, rejuvenation, and memory in active systems. The left axis represents a thermal cycle, and the right axis shows an activity cycle.

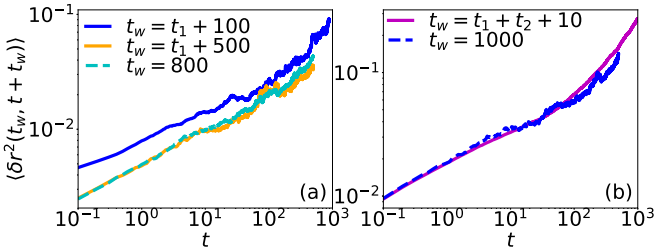


FIG. 2. Mean-squared displacements as a function of time for an active thermal system with a relatively small persistence time of $\tau_r = 1$, subjected to a thermal cycle. Panels (a) and (b) correspond to the second and third step of the thermal cycling protocol to probe rejuvenation and memory effects, respectively. In both panels solid lines correspond to different waiting times t_w (with $t_1 = t_2 = 1000$). The dashed curve in panel (a) corresponds to a direct quench to T_{q_2}, i.e., without the first aging step, at $t_w = 800$; the dashed curve in panel (b) corresponds to the end of the first step, $t_w = 1000$.

use $t_1 = t_2 = t_3 = 500$. We note that as an alternative active cycling protocol, one could also quench the self-propulsion force f. We have verified that by using the self-propulsion force as the control parameter instead of the persistence time, similar results are found (see Appendix).

To probe possible rejuvenation and memory effects, we analyze the mean-squared displacement $\langle \delta r^2(t_w, t + t_w) \rangle$ as a function of time t. The time t ranges from 0 to the duration of the protocol's steps, which is either 500 or 1000. The waiting time t_w is defined as the time elapsed after the start of the respective protocol. Explicitly, in the first step or in a direct quench, t_w represents the time spent at the first quenching temperature T_{q_1} or the quenched persistence time τ_{r_1}. In the second and third steps of the protocol, t_w is defined as $t_1 + \hat{t}_w$ and $t_1 + t_2 + \hat{t}_w$, respectively. Here, $0 \leqslant \hat{t}_w < 1000$ when the duration of each step is 1000, or $0 \leqslant \hat{t}_w < 500$ when the duration of each step is 500.

III. RESULTS AND DISCUSSION

A. Rejuvenation by thermal cycling: Active versus passive

We first discuss the results of thermal cycling applied to either an active or passive thermal system. The initial step of our thermal cycling protocol (step 1 in Fig. 1) corresponds to a temperature quench from high ($T_i = 1$) to low temperature ($T_{q_1} = 0.25$), which induces simple aging. As expected, during this aging step, the relaxation dynamics slows down with increasing waiting time t_w. Specifically, both the active and passive systems exhibit a power-law scaling of the structural relaxation time with respect to the waiting time, $\tau_\alpha \sim t_w^{-\delta}$, where the exponent δ is different for active and passive systems. These aging results are in full agreement with literature, both for the passive and active case [5,72,74].

The second step of the protocol (step 2 in Fig. 1) corresponds to a quench from $T_{q_1} = 0.25$ to $T_{q_2} = 0.1$, which may induce rejuvenation. Previous studies of passive systems [27,36] have shown that the rejuvenation effect is affected by both the temperature difference between the first and the second step $\Delta T = |T_{q_1} - T_{q_2}|$ and the duration of each step of the process. If t_1 is not long enough, an additional aging contribution may be observed. Testing the protocol with $t_1 = t_2 = 500$, we have found no evidence of rejuvenation in either the passive or active system (see Appendix). Indeed, during the second step of the process, with $T_{q_2} = 0.1$, the mean-squared displacement does not evolve as the system ages. This behavior could be due to a too-short time duration or a too-small ΔT. To investigate which of these parameters is responsible for this behavior, we repeat the protocol with $t_1 = t_2 = 1000$.

As shown in the Appendix, in the passive case, even with a longer duration of each step ($t_1 = 1000$), the system remains frozen at the new temperature $T_{q_2} = 0.1$, and the rejuvenation effect is not observed. Different waiting times $\hat{t}_w$ exhibit the same dynamical behavior, indicating that the aging dynamics is slowed down by this additional temperature quench [41]. These results are in agreement with existing literature showing that structural glasses display rejuvenation only when the duration of the first step is substantial ($t_1 = 1.2 \times 10^6$ or ∞ in Ref. [36]) and there is a considerable temperature jump between the steps. For spin glasses, especially in three dimensions, rejuvenation is also notoriously difficult to observe in simulations and typically requires an exceptionally large temperature jump [34]. Hence, in our case we believe the absence of rejuvenation in the passive glass may be attributed to either a time duration t_1 that is still too short or a ΔT that is not sufficiently large. However, decreasing the temperature T_{q_2} or further increasing t_1 is computationally expensive as the dynamics become noisier, and obtaining reliable results would require even more than 1000 independent configurations.

Conversely, for the active system, we do observe a rejuvenation effect under the same thermal cycling protocol. To see this, let us first consider an active system with a relatively small persistence time of $\tau_r = 1$. In Fig. 2(a) we plot the mean-squared displacements for this active system during the second step of the cycle for waiting times $t_w = t_1 + \hat{t}_w$, with $t_1 = 1000$ and $\hat{t}_w = 100, 500$. For comparison we also show the dynamics following a direct quench to the same temperature, $T_q = T_{q_2} = 0.1$. Notably, we observe that the mean-squared displacement at $t_w = t_1 + 500$ overlaps almost perfectly with that of a directly quenched sample at $t_w = 800$. This is the hallmark of rejuvenation: even though the system during the second step of the cycle is older (age $t_w = 1500$), it

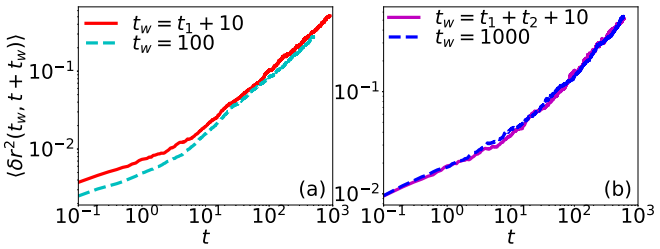


FIG. 3. Mean-squared displacements as a function of time for an active thermal system with a relatively large persistence time of $\tau_r = 10$, subjected to a thermal cycle. Panels (a) and (b) correspond to the second and third step of the thermal cycling protocol to probe rejuvenation and memory effects, respectively. In both panels, solid lines correspond to different waiting times t_w (with $t_1 = t_2 = 1000$). The dashed curve in panel (a) corresponds to a direct quench to T_{q_2}, i.e., without the first aging step, at $t_w = 100$; the dashed curve in panel (b) corresponds to the end of the first step, $t_w = 1000$.

behaves effectively as a younger system (age $t_w = 800$) that was quenched to the same temperature. Since the behavior obtained from a thermal cycle at waiting time $t_1 + \hat{t}_w$ is equivalent to a direct quench at waiting time t_w, this implies that the effective age of the system during the second step is $t_w^{eff} = t_w$. Consequently, in this case the effective waiting time can be expressed as $t_w^{eff} = \hat{t}_w + t^{ag}$, where t^{ag} is nonzero but smaller than t_1 (in this case $t_w^{eff} = 800$ and $t^{ag} = 300$). Note that the limiting case of $t^{ag} = 0$ would indicate perfect rejuvenation, i.e., as if the first aging step never happened.

To further investigate the rejuvenation effect in active systems, we consider a larger persistence time of $\tau_r = 10$. Figure 3(a) shows the corresponding mean-squared displacements at a waiting time $t_w = t_1 + 10$ during the second step of the cycle and at a waiting time $t_w = 100$ following a direct quench to the same temperature T_{q_2}. When comparing the two curves, we find that the short-time behavior of the mean-squared displacements at $t_w = t_1 + 10$ and $t_w = 100$ differs, in particular, the system in the second step is initially faster than a direct quench. Consequently, the short-time dynamics is still influenced by the first step of the protocol. However, the long-time behaviors of the mean-squared displacements at $t_w = t_1 + 10$ and $t_w = 100$ overlap. Therefore, we can conclude that increasing the persistence time in active systems leads to a "stronger" rejuvenation effect. In this case the extra aging contribution t^{ag} remains present but is smaller compared to that observed for the system with the smaller persistence time of $\tau_r = 1$. As a result, the system with $\tau_r = 10$ is effectively younger than the system with $\tau_r = 1$.

Overall, our results of the second step show that an active glassy system exhibits rejuvenation under thermal cycling, while its passive counterpart exposed to the same protocol does not. However, it must be noted that the rejuvenation process is "weak" in the sense that the material is still effectively older than a system subjected to a direct quench. In other words, the effect of the first aging step is still noticeable in the dynamics. We hypothesize that the active rejuvenation effect is due to the ability of self-propelling particles to escape their cages relatively easily, thus allowing them to effectively restart aging at the new temperature. To rationalize the importance of the persistence time on the rejuvenation dynamics, we note that the dynamics of a thermal active glass is governed by both thermal and active effects. On sufficiently long timescales, however, it is known that the activity becomes dominant [72] and hence systems with larger persistence times exhibit stronger rejuvenation effects.

B. Memory by thermal cycling: Active versus passive

Let us now look at the emergence of memory effects due to a temperature cycle. Such memory effects can occur in the final step of the thermal cycling protocol (step 3 in Fig. 1), in which the temperature is raised from $T_{q_2} = 0.1$ to $T_{q_1} = 0.25$. Figures 2(b) and 3(b) show the mean-squared displacements for two active systems with $\tau_r = 1$ and 10, respectively, at $t_w = t_1 + t_2 + 10$ (third step of the cycle) and $t_w = 1000$ (at the end of the first step). In both cases the results reveal that the system recovers the same behavior observed at the end of the first step after a waiting time $\hat{t}_w = 10$. Thus, for the waiting time $t_w^{mem} = t_1 + t_2 + t^*$, the system retains a memory of the time spent at T_{q_1}. However, due to the relatively small value of $t^* = 10$ (for both $\tau_r = 1$ and 10), the memory is not perfect, and this is the only consequence of the time spent at T_{q_2}. This behavior is consistent with previous results obtained in (passive) spin glasses [35,39], where it was shown that the time needed to remember the time spent at T_{q_1} is much shorter compared to the time spent at T_{q_2}, and hence, after a very brief transient, the dynamics continues as if the second step has never occurred. Moreover, our results indicate that, unlike the rejuvenation effect, the memory effect is independent of the persistence time. In order to achieve full memory, i.e., $t^* = 0$, we hypothesize that the temperature jump ΔT should be increased, as it has been shown in spin glasses that increasing ΔT leads to a decrease in t^* [35,39].

As shown in the Appendix, the memory effect can also be observed in passive systems, even when rejuvenation is absent. During the first step the dynamics is frozen at T_{q_2}, but shortly after the temperature is raised back to T_{q_1}, the passive system remembers its behavior during the first step. In a similar manner to the active case, the memory effect in passive systems also exhibits a small t^*, which represents the only consequence of the second step of the cycling. This suggests that, unlike rejuvenation, the memory effect is easier to observe in these systems. The presence of memory effects in these systems, even without rejuvenation, is consistent with the findings in the existing literature, where memory represents a common phenomenon observed in various systems. Such systems include materials experiencing cyclic deformation and biologically relevant systems like blood flow and growing tissue monolayers [79].

C. Rejuvenation and memory by active cycling: From active to passive

We now consider the activity cycling protocol that, in contrast to thermal cycling, can only be applied to active systems. Here it is instructive to note that the cyclic change of the ABP persistence time τ_r also corresponds to an *effective* temperature cycle [80]. Hence, this protocol offers not only a means to generate novel dynamics in active systems, but it also allows us to induce effectively large temperature jumps

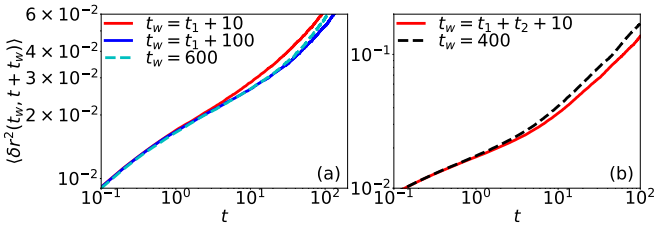


FIG. 4. Mean-squared displacements as a function of time for an active thermal system ($T = 0.25$, $f = 0.5$) subjected to an activity cycle. Panels (a) and (b) correspond to the second and third step of the active cycling protocol to probe rejuvenation and memory effects, respectively. In both panels, solid lines correspond to different waiting times t_w (with $t_1 = t_2 = 500$). The dashed curve in panel (a) corresponds to a direct quench to a passive system at $t_w = 600$; the dashed curve in panel (b) represents the mean-squared displacement before the end of the first step $t_w = 400$.

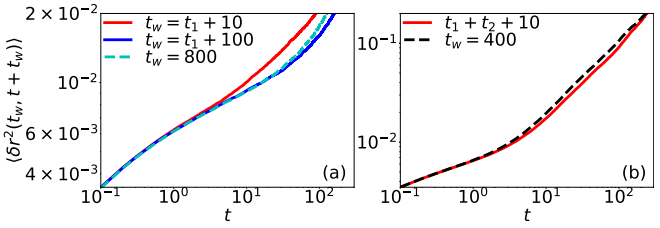


FIG. 5. Mean-squared displacements as a function of time for an active thermal system ($T = 0.1$, $f = 0.5$) subjected to an activity cycle. Panels (a) and (b) correspond to the second and third step of the active cycling protocol to probe rejuvenation and memory effects, respectively. In both panels, solid lines correspond to different waiting times t_w (with $t_1 = t_2 = 500$). The dashed curve in panel (a) corresponds to a direct quench to a passive system at $t_w = 800$; the dashed curve in panel (b) represents the mean-squared displacement before the end of the first step $t_w = 400$.

between steps via τ_r (while keeping T fixed). The latter aspect is particularly useful to induce rejuvenation on reasonable simulation timescales, as rejuvenation demands a large temperature difference between steps or long step durations (see Sec. III A).

During the first step of the activity cycle, we again observe simple aging, similar to the thermal cycling scenario. Figure 4(a) illustrates the mean-squared displacement in the second step of the activity cycling (i.e., where the persistence time is quenched to $\tau_{r_2} = 0$) at a fixed temperature of $T = 0.25$. Unlike thermal cycling, where the dynamics is frozen at $t_1 = 500$, in activity cycling the dynamics evolves for different $\hat{t}_w$. Notably, the aging restarts, and at a waiting time of approximately $t_w = t_1 + 100$, the system recovers the behavior observed after a direct quench at $\tau_{r_2} = 0$. The behavior in the second step overlaps with the one found with a direct quench for $t_w = 600$, thus indicating a rejuvenation effect. Here, since $t_1 = 500$ and $\hat{t}_w = 100$, we can conclude that applying a direct quench or an activity cycling is equivalent, but the first step of the cycling has an impact on the second step because $t^{ag} = t_1$. We have verified that the same rejuvenation behavior can be found when using the self-propulsion force as the control parameter instead of the persistence time (see Appendix). This indicates that this behavior is protocol independent, and quenching the self-propulsion force or the persistence time leads to the same dynamical behavior.

To understand if temperature plays a role in this weak rejuvenation effect, we repeat the activity cycling at a lower temperature of $T = 0.1$. Figure 5(a) shows the behavior of the system during the second step of the activity cycling at this lower temperature. We find that the behavior of the system at the second step at $t_w = t_1 + 100$ overlaps with that observed from a direct quench at $t_w = 800$. This indicates that the consequence of the first step of the cycle makes the system slightly older compared to a direct quench. This phenomenon is strongly reminiscent of so-called *overaging* in systems under shear [81,82], and here we also refer to systems that appear older than their simple-aging equivalent as being overaged. We can attribute the overaging effect to the fact that t_1 is not long enough. Comparing this activity cycling to thermal cycling, we observe that the short duration of the first step leads to overaging and freezing of the dynamics, respectively. In conclusion, the observation of nonequilibrium phenomena such as rejuvenation becomes more accessible when activity cycling is applied. This is attributed to the significantly larger effective temperature jump compared to a purely passive system undergoing thermal cycling.

Finally, as shown in Figs. 4(b) and 5(b), in the third step, when the persistence time is raised again to $\tau_{r_1} = 10$, the system quickly recovers the same behavior found at the end of the first step. Consequently, the system has a memory of the first step as if the second step did not happen. In agreement with the thermal cycle, the system needs a time t^* to "remember" the time spent at τ_{r_1}. The presence of this t^* can be due to the fact that the duration of each step of the cycle is not long enough. Therefore we conclude that when applying an active cycle, we observe memory effects. We have also verified that this memory effect is present when the control parameter of the activity cycle is the self-propulsion force (see Appendix). In contrast to the rejuvenation effect, the memory effect found within the activity cycle is consistent with that observed when thermal cycling is applied.

IV. CONCLUSIONS

In summary, our work reveals that the nonequilibrium dynamic behaviors caused by a temperature cycle in an active thermal system are significantly different from those in a passive system. Specifically, an active system subjected to a temperature cycle exhibits rejuvenation and memory effects, whereas in the passive case, the system gets frozen at the new temperature and the rejuvenation effect is absent [41]. Nevertheless, even in the absence of rejuvenation in the passive case, a memory effect similar to that observed in the active system can still be found. Additionally, we find that the rejuvenation effect becomes stronger as the persistence time increases, whereas the memory effect is independent of this parameter. We can rationalize the enhanced rejuvenation of more persistent active particles by considering that the long-time behavior of active thermal glasses is dominated by activity rather than thermal motion [72]. Hence, a more active system with a larger persistence time will more easily restart

the aging process after a sudden temperature change, leading to a "stronger" rejuvenation effect.

We find that rejuvenation and memory effects in active matter can also be induced by a nonequilibrium protocol unique to active systems, namely, via an activity cycle. In particular, the application of an activity cycle from an active to a passive system enables access to higher temperature jumps without increasing the noise, leading to rejuvenation. Depending on the temperature of the system, we can observe either rejuvenation or overaging, with the latter occurring at lower temperatures. To mitigate the overaging effect at low temperatures, it is necessary to increase the duration of the first step of the protocol. Overall, our findings suggest that activity cycling offers richer nonequilibrium dynamics in the second step of the cycle compared to thermal cycling, when the duration of the first step is short. Moreover, even with this protocol, the memory of the first step of the cycle is quickly recovered when the system becomes active again. Our results also demonstrate that similar outcomes can be achieved by employing the self-propulsion force as the control parameter in the activity cycle. Moreover, these findings align with prior research indicating that different protocols yield comparable dynamics. This similarity is reminiscent of quenching protocols employed to study simple aging, where an activity quench generates analogous outcomes to a temperature quench [72,74].

Our study provides insights into the rich nonequilibrium dynamics of active glasses and emphasizes the significance of exploring the interplay between temperature and activity. Furthermore, our results show that although the nature of an active system differs from that of spin glasses, the out-of-equilibrium dynamics observed during a temperature cycle exhibit remarkable similarities. The rejuvenation and memory effects observed in spin glasses have been attributed to the slow increase of a characteristic length following a temperature quench [17–19], or explained using a hierarchical energy-landscape picture [20,21,83–85]. However, since active systems are non-Hamiltonian and are not governed by energy minimization, understanding the presence of rejuvenation and memory effects in these systems will require a different theoretical framework. Finally, given that dense active matter is becoming increasingly relevant in the context of biology, it will be interesting to explore in future work how physical aging, rejuvenation, and memory are manifested in biological glassy systems such as confluent cell layers, tissues, and solid tumors [59,67,70,86–89].

ACKNOWLEDGMENTS

We thank K. Storm for his critical reading of the manuscript. This work has been financially supported by the Dutch Research Council (NWO) through a Physics Projectruimte grant.

APPENDIX

1. Thermal Cycling

In Figs. 6 and 7 we present the mean-squared displacements for a passive system and an active system ($f = 0.5$ and $\tau_r = 1$), respectively, subjected to thermal cycling with

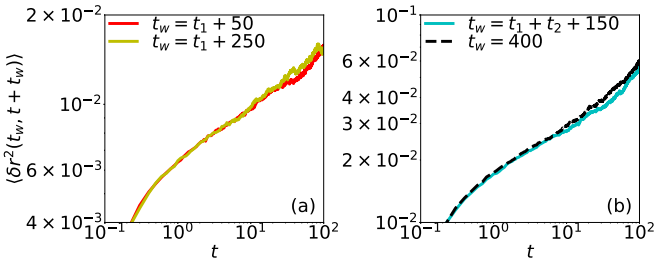


FIG. 6. Mean-squared displacements as a function of time for a passive system, subjected to a thermal cycle with $t_1 = t_2 = t_3 = 500$. Panels (a) and (b) correspond to the second and third step of the thermal cycling protocol to probe rejuvenation and memory effects, respectively. In both panels, solid lines correspond to different waiting times t_w. The dashed curve in panel (b) represents the mean-squared displacement before the end of the first step, at $t_w = 400$.

$t_1 = t_2 = t_3 = 500$. Figures 6(a) and 7(a) show the results of the second step of the thermal cycling. It can be seen that different waiting times $\hat{t}_w$ yield virtually the same dynamical behavior, which is a manifestation of the fact that both systems are frozen at the new temperature T_{q_2}. Hence, there is no rejuvenation effect in this case. On the other hand, in Figs. 6(b) and 7(b) we clearly observe that the memory effect is present in the third step of the cycle.

Figure 8 shows the mean-squared displacement for a passive system subjected to thermal cycling with $t_1 = t_2 = t_3 = 1000$. In Fig. 8(a) it is evident that even with a longer time duration for the first step, the passive system does not rejuvenate; instead, the dynamics remains frozen at the new temperature. However, in the third step of the cycle, as shown in Fig. 8(b), after a short transient the system "remembers" the time spent at T_{q_1}, as if the second step of the cycle never occurred.

2. Active Cycling

Here we present the results of an activity cycle in which the self-propulsion force f is varied while keeping the temperature and persistence time constant at $T = 0.25$ and $\tau_r = 1$,

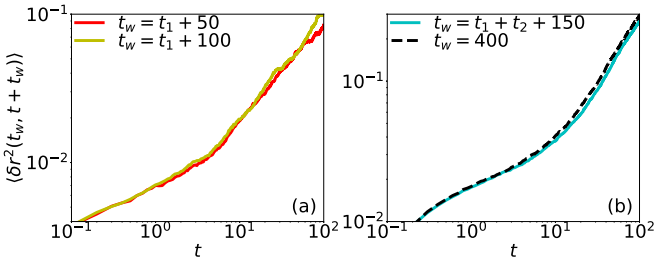


FIG. 7. Mean-squared displacements as a function of time for an active system with $\tau_r = 1$, subjected to a thermal cycle with $t_1 = t_2 = t_3 = 500$. Panels (a) and (b) correspond to the second and third step of the thermal cycling protocol to probe rejuvenation and memory effects, respectively. In both panels, solid lines correspond to different waiting times t_w. The dashed curve in panel (b) represents the mean-squared displacement before the end of the first step, at $t_w = 400$.

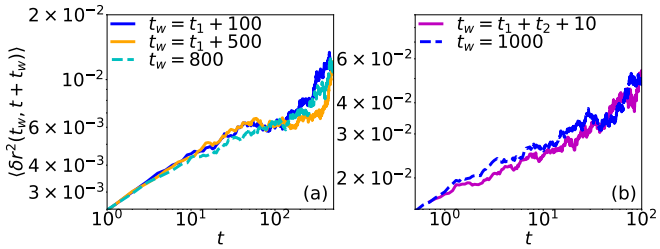


FIG. 8. Mean-squared displacements as a function of time for a passive system, subjected to a thermal cycle with $t_1 = t_2 = t_3 = 1000$. Panels (a) and (b) correspond to the second and third step of the thermal cycling protocol to probe rejuvenation and memory effects, respectively. In both panels, solid lines correspond to different waiting times t_w. The dashed curve in panel (a) corresponds to a direct quench to T_{q_2}, i.e., without the first aging step, at $t_w = 800$; the dashed curve in panel (b) corresponds to the end of the first step, at $t_w = 1000$.

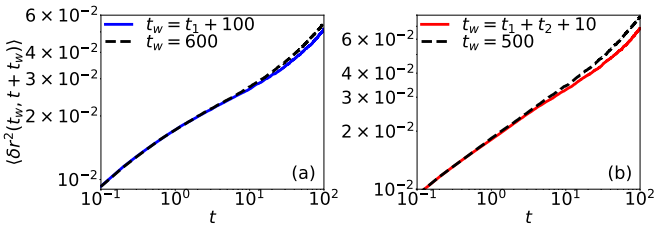


FIG. 9. Mean-squared displacements as a function of time for an active thermal system ($T = 0.25$, $\tau_r = 1$) subjected to an activity cycle in which the active force f is changed. Panels (a) and (b) correspond to the second and third step of the active cycling protocol to probe rejuvenation and memory effects, respectively. In both panels, solid lines correspond to different waiting times t_w (with $t_1 = t_2 = 500$). The dashed curve in panel (a) corresponds to a direct quench to a passive system at $t_w = 600$; the dashed curve in panel (b) represents the mean-squared displacement before the end of the first step, at $t_w = 400$.

respectively. The activity cycle proceeds as follows: We first equilibrate the system at an activity of $f_{q_i} = 5$, then quench the activity to $f_{q_1} = 0.5$, and allow the system to evolve for a time interval of $t_1 = 500$. After this period we quench the activity once again to $f_{q_2} = 0$, and after a time interval of $t_2 = t_1$, we increase the activity back to $f_{q_1} = 0.5$.

Figure 9 shows the mean-squared displacement for an active system subjected to the above activity cycling protocol with $t_1 = t_2 = t_3 = 500$. Similar to the results obtained in the main text when the control parameter is the persistence time, in the second step of the cycle [Fig. 9(a)], the system at $t_w = t_1 + 100$ recovers the behavior obtained from a direct quench at $t_w = 600$. This is indicative of rejuvenation. In the third step of the cycle, as shown in Fig. 9(b), the system recovers the behavior observed at the end of the first step, thus exhibiting memory.

[1] K. Binder and W. Kob, *Glassy Materials and Disordered Solids: An Introduction to Their Statistical Mechanics* (World Scientific, Singapore, 2011).

[2] G. Biroli and J. P. Garrahan, Perspective: The glass transition, J. Chem. Phys. **138**, 12A301 (2013).

[3] P. G. Debenedetti and F. H. Stillinger, Supercooled liquids and the glass transition, Nature (London) **410**, 259 (2001).

[4] F. Turci, C. P. Royall, and T. Speck, Nonequilibrium phase transition in an atomistic glassformer: The connection to thermodynamics, Phys. Rev. X **7**, 031028 (2017).

[5] W. Kob and J. L. Barrat, Aging effects in a Lennard-Jones glass, Phys. Rev. Lett. **78**, 4581 (1997).

[6] G. Foffi, E. Zaccarelli, S. Buldyrev, F. Sciortino, and P. Tartaglia, Aging in short-ranged attractive colloids: A numerical study, J. Chem. Phys. **120**, 8824 (2004).

[7] I. M. Hodge, Physical aging in polymer glasses, Science **267**, 1945 (1995).

[8] L. Berthier and G. Biroli, A statistical mechanics perspective on glasses and aging, in *Encyclopedia of Complexity and Systems Science*, edited by R. A Meyers (Springer, 2009), p. 4209.

[9] P. Lunkenheimer, R. Wehn, U. Schneider, and A. Loidl, Glassy aging dynamics, Phys. Rev. Lett. **95**, 055702 (2005).

[10] J. Zhao, S. L. Simon, and G. B. McKenna, Using 20-million-year-old amber to test the super-Arrhenius behaviour of glass-forming systems, Nat. Commun. **4**, 1783 (2013).

[11] J. Y. Raty, W. Zhang, J. Luckas, C. Chen, R. Mazzarello, C. Bichara, and M. Wuttig, Aging mechanisms in amorphous phase-change materials, Nat. Commun. **6**, 7467 (2015).

[12] P. Wang, C. Song, and H. A. Makse, Dynamic particle tracking reveals the ageing temperature of a colloidal glass, Nat. Phys. **2**, 526 (2006).

[13] G. Odegard and A. Bandyopadhyay, Physical aging of epoxy polymers and their composites, J. Polym. Sci., Part B: Polym. Phys. **49**, 1695 (2011).

[14] B. Martin, Aging and strength of bone as a structural material, Calcif. Tissue Int. **53**, S34 (1993).

[15] G. B. McKenna, Y. Leterrier, and C. R. Schultheisz, The evolution of material properties during physical aging, Polym. Eng. Sci. **35**, 403 (1995).

[16] L. C. E. Struik, Physical aging in plastics and other glassy materials, Polym. Eng. Sci. **17**, 165 (1977).

[17] D. S. Fisher and D. A. Huse, Nonequilibrium dynamics of spin glasses, Phys. Rev. B **38**, 373 (1988).

[18] G. Koper and H. Hilhorst, A domain theory for linear and nonlinear aging effects in spin glasses, J. Phys. **49**, 429 (1988).

[19] A. J. Bray and M. A. Moore, Chaotic nature of the spin-glass phase, Phys. Rev. Lett. **58**, 57 (1987).

[20] M. Mézard, G. Parisi, and M. A. Virasoro, *Spin Glass Theory and Beyond: An Introduction to the Replica Method and Its Applications*, Vol. 9 (World Scientific Publishing Company, Singapore, 1987).

[21] Y. Jin and H. Yoshino, Exploring the complex free-energy landscape of the simplest glass by rheology, Nat. Commun. **8**, 14935 (2017).

[22] K. Jonason, E. Vincent, J. Hammann, J. P. Bouchaud, and P. Nordblad, Memory and chaos effects in spin glasses, Phys. Rev. Lett. **81**, 3243 (1998).

[23] L. Lundgren, P. Svedlindh, P. Nordblad, and O. Beckman, Dynamics of the relaxation-time spectrum in a CuMn spin-glass, Phys. Rev. Lett. **51**, 911 (1983).

[24] J. O. Andersson, J. Mattsson, and P. Nordblad, Overlap length in a Cu-Mn spin glass probed by ac susceptibility, Phys. Rev. B **48**, 13977 (1993).

[25] V. Dupuis, E. Vincent, J.-P. Bouchaud, J. Hammann, A. Ito, and H. A. Katori, Aging, rejuvenation, and memory effects in Ising and Heisenberg spin glasses, Phys. Rev. B **64**, 174204 (2001).

[26] P. E. Jönsson, H. Yoshino, and P. Nordblad, Symmetrical temperature-chaos effect with positive and negative temperature shifts in a spin glass, Phys. Rev. Lett. **89**, 097201 (2002).

[27] L. Berthier and J.-P. Bouchaud, Geometrical aspects of aging and rejuvenation in the Ising spin glass: A numerical study, Phys. Rev. B **66**, 054404 (2002).

[28] L. Berthier and A. P. Young, Aging dynamics of the Heisenberg spin glass, Phys. Rev. B **69**, 184423 (2004).

[29] L. Berthier and A. P. Young, Temperature cycles in the Heisenberg spin glass, Phys. Rev. B **71**, 214429 (2005).

[30] J.-P. Bouchaud, V. Dupuis, J. Hammann, and E. Vincent, Separation of time and length scales in spin glasses: Temperature as a microscope, Phys. Rev. B **65**, 024439 (2001).

[31] J.-P. Bouchaud and G. Biroli, Nonlinear susceptibility in glassy systems: A probe for cooperative dynamical length scales, Phys. Rev. B **72**, 064204 (2005).

[32] K. Jonason, P. Nordblad, E. Vincent, J. Hammann, and J.-P. Bouchaud, Memory interference effects in spin glasses, Eur. Phys. J. B **13**, 99 (2000).

[33] M. Sasaki, V. Dupuis, J.-P. Bouchaud, and E. Vincent, Deviations from perfect memory in spin glass temperature cycling experiments, Eur. Phys. J. B **29**, 469 (2002).

[34] M. Baity-Jesi, E. Calore, A. Cruz, L. A. Fernandez, J. M. Gil-Narvion, I. Gonzalez-Adalid Pemartin, A. Gordillo-Guerrero, D. Iñiguez, A. Maiorano, E. Marinari, V. Martin-Mayor, J. Moreno-Gordo, A. Muñoz Sudupe, D. Navarro, I. Paga, G. Parisi, S. Perez-Gaviro, F. Ricci-Tersenghi, J. J. Ruiz-Lorenzo, S. F. Schifano *et al.*, Memory and rejuvenation effects in spin glasses are governed by more than one length scale, Nat. Phys. **19**, 978 (2023).

[35] E. Vincent, Ageing, rejuvenation and memory: The example of spin-glasses, in *Ageing and the Glass Transition*, edited by M. Henkel, M. Pleimling, and R. Sanctuary (Springer, Berlin, Heidelberg, 2007), pp. 7–60.

[36] C. Scalliet and L. Berthier, Rejuvenation and memory effects in a structural glass, Phys. Rev. Lett. **122**, 255502 (2019).

[37] F. Lefloch, J. Hammann, M. Ocio, and E. Vincent, Can aging phenomena discriminate between the droplet model and a hierarchical description in spin glasses? Europhys. Lett. **18**, 647 (1992).

[38] M. Bruns and F. Varnik, Rejuvenation in deep thermal cycling of a generic model glass: A study of per-particle energy distribution, Materials **15**, 829 (2022).

[39] E. Vincent, J. Bouchaud, J. Hammann, and F. Lefloch, Contrasting effects of field and temperature variations on ageing in spin glasses, Philos. Mag. B **71**, 489 (1995).

[40] N. V. Priezjev, The effect of cryogenic thermal cycling on aging, rejuvenation, and mechanical properties of metallic glasses, J. Non-Cryst. Solids **503-504**, 131 (2019).

[41] M. Bruns, M. Hassani, F. Varnik, A. Hassanpour, S. Divinski, and G. Wilde, Decelerated aging in metallic glasses by low temperature thermal cycling, Phys. Rev. Res. **3**, 013234 (2021).

[42] B. Shang, W. Wang, A. L. Greer, and P. Guan, Atomistic modelling of thermal-cycling rejuvenation in metallic glasses, Acta Mater. **213**, 116952 (2021).

[43] J. Ketkaew, R. Yamada, H. Wang, D. Kuldinow, B. S. Schroers, W. Dmowski, T. Egami, and J. Schroers, The effect of thermal cycling on the fracture toughness of metallic glasses, Acta Mater. **184**, 100 (2020).

[44] Q.-L. Liu and N. V. Priezjev, The influence of complex thermal treatment on mechanical properties of amorphous materials, Comput. Mater. Sci. **161**, 93 (2019).

[45] S. V. Ketov, Y. H. Sun, S. Nachum, Z. Lu, A. Checchi, A. R. Beraldin, H. Y. Bai, W. H. Wang, D. V. Louzguine-Luzgin, M. A. Carpenter, and A. L. Greer, Rejuvenation of metallic glasses by non-affine thermal strain, Nature (London) **524**, 200 (2015).

[46] W. Guo, R. Yamada, and J. Saida, Rejuvenation and plasticization of metallic glass by deep cryogenic cycling treatment, Intermetallics **93**, 141 (2018).

[47] Y. Tong, T. Iwashita, W. Dmowski, H. Bei, Y. Yokoyama, and T. Egami, Structural rejuvenation in bulk metallic glasses, Acta Mater. **86**, 240 (2015).

[48] G. Szamel, Theory for the dynamics of dense systems of athermal self-propelled particles, Phys. Rev. E **93**, 012603 (2016).

[49] M. Feng and Z. Hou, Mode coupling theory for nonequilibrium glassy dynamics of thermal self-propelled particles, Soft Matter **13**, 4464 (2017).

[50] A. Liluashvili, J. Ónody, and T. Voigtmann, Mode-coupling theory for active Brownian particles, Phys. Rev. E **96**, 062608 (2017).

[51] S. Henkes, Y. Fily, and M. C. Marchetti, Active jamming: Self-propelled soft particles at high density, Phys. Rev. E **84**, 040301(R) (2011).

[52] R. Ni, M. A. C. Stuart, and M. Dijkstra, Pushing the glass transition towards random close packing using self-propelled hard spheres, Nat. Commun. **4**, 2704 (2013).

[53] L. Berthier and J. Kurchan, Non-equilibrium glass transitions in driven and active matter, Nat. Phys. **9**, 310 (2013).

[54] L. Berthier, Nonequilibrium glassy dynamics of self-propelled hard disks, Phys. Rev. Lett. **112**, 220602 (2014).

[55] G. Szamel, E. Flenner, and L. Berthier, Glassy dynamics of athermal self-propelled particles: Computer simulations and a nonequilibrium microscopic theory, Phys. Rev. E **91**, 062304 (2015).

[56] E. Flenner, G. Szamel, and L. Berthier, The nonequilibrium glassy dynamics of self-propelled particles, Soft Matter **12**, 7136 (2016).

[57] L. Berthier, E. Flenner, and G. Szamel, How active forces influence nonequilibrium glass transitions, New J. Phys. **19**, 125006 (2017).

[58] M. Scholz, S. Burov, K. L. Weirich, B. J. Scholz, S. M. Ali Tabei, M. L. Gardel, and A. R. Dinner, Cycling state that can lead to glassy dynamics in intracellular transport, Phys. Rev. X **6**, 011037 (2016).

[59] L. M. C. Janssen, Active glasses, J. Phys.: Condens. Matter **31**, 503002 (2019).

[60] L. Berthier, E. Flenner, and G. Szamel, Glassy dynamics in dense systems of active particles, J. Chem. Phys. **150**, 200901 (2019).

[61] C. Lozano, J. R. Gomez-Solano, and C. Bechinger, Active particles sense micromechanical properties of glasses, Nat. Mater. **18**, 1118 (2019).

[62] N. Klongvessa, F. Ginot, C. Ybert, C. Cottin-Bizonne, and M. Leocmach, Active glass: Ergodicity breaking dramatically affects response to self-propulsion, Phys. Rev. Lett. **123**, 248004 (2019).

[63] N. Klongvessa, F. Ginot, C. Ybert, C. Cottin-Bizonne, and M. Leocmach, Nonmonotonic behavior in dense assemblies of active colloids, Phys. Rev. E **100**, 062603 (2019).

[64] D. Bi, J. H. Lopez, J. M. Schwarz, and M. L. Manning, A density-independent rigidity transition in biological tissues, Nat. Phys. **11**, 1074 (2015).

[65] D. Needleman and Z. Dogic, Active matter at the interface between materials science and cell biology, Nat. Rev. Mater. **2**, 17048 (2017).

[66] B. R. Parry, I. V. Surovtsev, M. T. Cabeen, C. S. O'Hern, E. R. Dufresne, and C. Jacobs-Wagner, The bacterial cytoplasm has glass-like properties and is fluidized by metabolic activity, Cell **156**, 183 (2014).

[67] S. Garcia, E. Hannezo, J. Elgeti, J.-F. Joanny, P. Silberzan, and N. S. Gov, Physics of active jamming during collective cellular motion in a monolayer, Proc. Natl. Acad. Sci. USA **112**, 15314 (2015).

[68] D. Bi, X. Yang, M. C. Marchetti, and M. L. Manning, Motility-driven glass and jamming transitions in biological tissues, Phys. Rev. X **6**, 021011 (2016).

[69] K. Nishizawa, K. Fujiwara, M. Ikenaga, N. Nakajo, M. Yanagisawa, and D. Mizuno, Universal glass-forming behavior of in vitro and living cytoplasm, Sci. Rep. **7**, 15143 (2017).

[70] T. E. Angelini, E. Hannezo, X. Trepat, M. Marquez, J. J. Fredberg, and D. A. Weitz, Glass-like dynamics of collective cell migration, Proc. Natl. Acad. Sci. **108**, 4714 (2011).

[71] J. Zhang, R. Alert, J. Yan, N. S. Wingreen, and S. Granick, Active phase separation by turning towards regions of higher density, Nat. Phys. **17**, 961 (2021).

[72] G. Janzen and L. M. C. Janssen, Aging in thermal active glasses, Phys. Rev. Res. **4**, L012038 (2022).

[73] L. M. C. Janssen, A. Kaiser, and H. Löwen, Aging and rejuvenation of active matter under topological constraints, Sci. Rep. **7**, 5667 (2017).

[74] R. Mandal and P. Sollich, Multiple types of aging in active glasses, Phys. Rev. Lett. **125**, 218001 (2020).

[75] W. Kob and H. C. Andersen, Testing mode-coupling theory for a supercooled binary Lennard-Jones mixture I: The Van Hove correlation function, Phys. Rev. E **51**, 4626 (1995).

[76] S. Plimpton, Fast parallel algorithms for short-range molecular dynamics, J. Comput. Phys. **117**, 1 (1995).

[77] E. Flenner and G. Szamel, Fundamental differences between glassy dynamics in two and three dimensions, Nat. Commun. **6**, 7392 (2015).

[78] D. Li, H. Xu, and J. P. Wittmer, Glass transition of two-dimensional 80–20 Kob–Andersen model at constant pressure, J. Phys.: Condens. Matter **28**, 045101 (2016).

[79] S. R. Nagel, S. Sastry, Z. Zeravcic, and M. Muthukumar, Memory formation, J. Chem. Phys. **158**, 210401 (2023).

[80] C. Bechinger, R. Di Leonardo, H. Löwen, C. Reichhardt, G. Volpe, and G. Volpe, Active particles in complex and crowded environments, Rev. Mod. Phys. **88**, 045006 (2016).

[81] V. Viasnoff and F. Lequeux, Rejuvenation and overaging in a colloidal glass under shear, Phys. Rev. Lett. **89**, 065701 (2002).

[82] L. Berthier, V. Viasnoff, O. White, V. Orlyanchik, and F. Krzakala, in *Slow Relaxations and Nonequilibrium Dynamics in Condensed Matter*, edited by J.-L. Barrat, M. Feigelman, J. Kurchan, and J. Dalibard (Springer, Berlin, Heidelberg, 2003), pp. 719–742.

[83] G. Parisi, A sequence of approximated solutions to the *s-k* model for spin glasses, J. Phys. A: Math. Gen. **13**, L115 (1980).

[84] D. Sherrington and S. Kirkpatrick, Solvable model of a spin-glass, Phys. Rev. Lett. **35**, 1792 (1975).

[85] P. Sibani and K. H. Hoffmann, Hierarchical models for aging and relaxation of spin glasses, Phys. Rev. Lett. **63**, 2853 (1989).

[86] E.-M. Schoetz, M. Lanio, J. A. Talbot, and M. L. Manning, Glassy dynamics in three-dimensional embryonic tissues, J. R. Soc. Interface **10**, 20130726 (2013).

[87] L. Atia, J. J. Fredberg, N. S. Gov, and A. F. Pegoraro, Are cell jamming and unjamming essential in tissue development? Cells Dev. **168**, 203727 (2021).

[88] F. Sauer, A. Fritsch, S. Grosser, S. Pawlizak, T. Kießling, M. Reiss-Zimmermann, M. Shahryari, W. C. Müller, K.-T. Hoffmann, J. A. Käs, and I. Sack, Whole tissue and single cell mechanics are correlated in human brain tumors, Soft Matter **17**, 10744 (2021).

[89] P. Gottheil, J. Lippoldt, S. Grosser, F. Renner, M. Saibah, D. Tschodu, A.-K. Poßögel, A.-S. Wegscheider, B. Ulm, K. Friedrichs, C. Lindner, C. Engel, M. Löffler, B. Wolf, M. Höckel, B. Aktas, H. Kubitschke, A. Niendorf, and J. A. Käs, State of cell unjamming correlates with distant metastasis in cancer patients, Phys. Rev. X **13**, 031003 (2023).